

We are IntechOpen, the world's leading publisher of Open Access books Built by scientists, for scientists

6,900

Open access books available

186,000

International authors and editors

200M

Downloads

Our authors are among the

154

Countries delivered to

TOP 1%

most cited scientists

12.2%

Contributors from top 500 universities



WEB OF SCIENCE™

Selection of our books indexed in the Book Citation Index
in Web of Science™ Core Collection (BKCI)

Interested in publishing with us?
Contact book.department@intechopen.com

Numbers displayed above are based on latest data collected.
For more information visit www.intechopen.com



Annexin A1-Binding Carbohydrate Mimetic Peptide Targets Drugs to Brain Tumors

Michiko N. Fukuda, Misa Suzuki-Anekoji
and Motohiro Nonaka

Abstract

Annexin A1 (Anxa1) is expressed specifically on the surface of the tumor vasculature. Previously, we demonstrated that a carbohydrate-mimetic peptide, designated IF7, bound to the Anxa1 N-terminal domain. Moreover, intravenously injected IF7 targeted the tumor vasculature in mouse and crossed tumor endothelia cells to stroma via transcytosis. Thus, we hypothesized that IF7 could overcome the blood–brain barrier to reach brain tumors. Our studies in brain tumor model mice showed that IF7 conjugated with the anti-cancer drug SN38 suppressed brain tumor growth with high efficiency. Furthermore IF7-SN38-treated mice mounted an immune response to brain tumors established by injected tumor cells and shrank those tumors in part by recruiting cytotoxic T-cells to the injection site. These results suggest that Anxa1-binding peptide IF7 represents a drug delivery vehicle useful to treat malignant brain tumors. This chapter describes the unique development of IF7-SN38 as a potential breakthrough cancer chemotherapeutic.

Keywords: carbohydrate mimetic peptides, phage display, annexin 1(Anxa1), blood–brain barrier (BBB), glioblastoma, chemotherapy, SN-38, CPT-11, geldanamycin (GA), cytotoxic T cell, CD8

1. Introduction

Brain malignancies are difficult to treat due to the blood–brain barrier (BBB), a layer of endothelial cells that separates the circulation from the brain and protects the central nervous system from pathogens and toxic materials [1, 2]. Although brain tumor cells cultured *in vitro* respond to several anti-cancer drugs, brain tumors *in vivo* do not due to the BBB. Chemotherapeutic drugs capable of passing the BBB are small lipophilic molecules of less than 500 Da [3], as exemplified by temozolomide [4–6]. Numerous investigators have attempted to overcome this hurdle using brain vasculature surface receptor-mediated proteins [7, 8], tumor-penetrating peptides [4, 9, 10], or nanoparticles [11, 12]. However, these attempts have not yet achieved clinically satisfactory results. On the other hand, tumor vasculature surrounding a brain tumor is chaotic, allowing large molecules and nanoparticles to overcome the BBB by passing through gaps between endothelial cells [13]. However, as this approach relies on passive diffusion, drugs must be administered at the maximum tolerable dose, causing adverse side effects.

Thus, efficient treatment of brain tumors requires both tumor vasculature targeting and penetration by a therapeutic to overcome the BBB. In this chapter, we describe the carbohydrate mimetic 7-mer peptide IF7, which serves as a highly specific tumor vasculature-targeting vehicle. When conjugated to the anti-cancer drug SN-38 and injected into mouse brain tumor models, IF7-SN38 has a potent anti-tumor effect. IF7-SN38 represents a potential breakthrough chemotherapeutic in brain malignancies.

2. IF7 peptide: how was it identified?

IF7 is a linear 7-mer peptide with the sequence IFLWQR [14]. This peptide is considered a carbohydrate mimetic, as it was identified in studies of cancer cell surface carbohydrates [15, 16]. Epithelial cancer cells express complex carbohydrate antigens, and some serve as ligands for carbohydrate binding proteins known as selectins. We hypothesized that interaction between selectin and selectin ligand functions in carbohydrate-dependent tumor cells colonization to the lung [17], in a manner similar to that seen in selectin-dependent hematogenous liver metastasis [18, 19].

Our goal, however, was challenging, as chemical synthesis of oligosaccharides as elaborate as the selectin ligand involved tedious, time-consuming and therefore expensive steps. To overcome this problem, we used phage display technology to identify carbohydrate mimetic peptides that might function as an E-selectin ligand. However, initially when we used E-selectin as the target, we did not obtain a phage clone. We then took a different approach and screened peptides for ability to bind

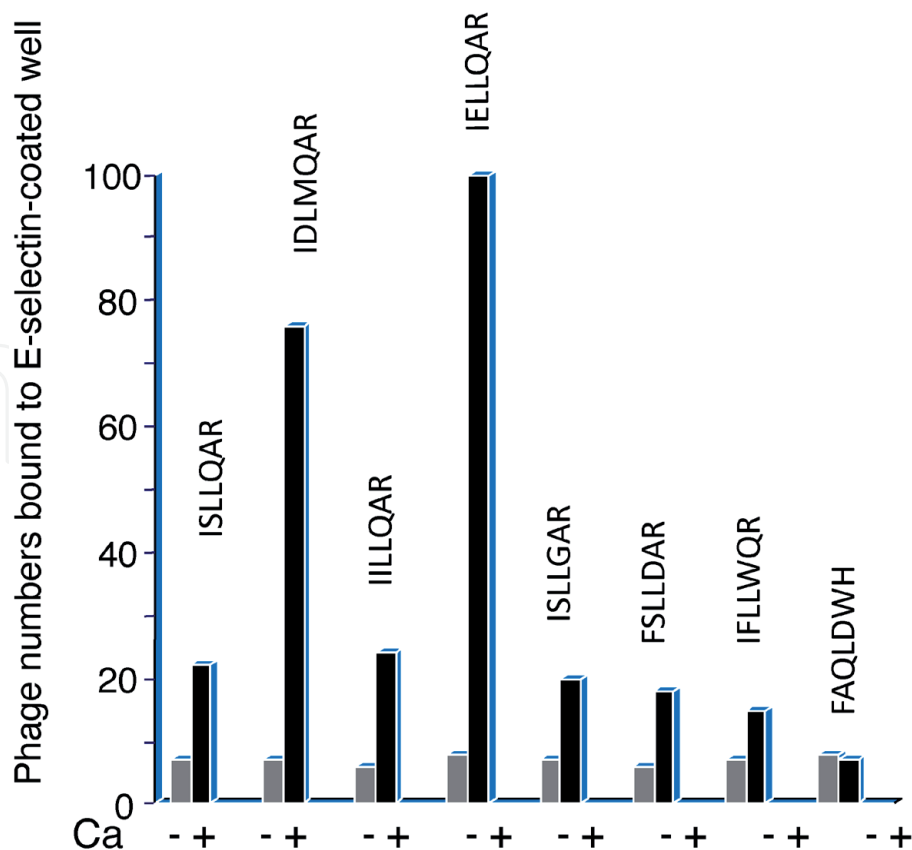


Figure 1.

E-selectin binding of linear 7-mer peptide sequences. Phage clones were selected by mouse monoclonal anti-Lewis A antibody (clone 7LE). Each cloned phage was added to microtiter plate wells coated with E-selectin-IgG chimeric protein. Phage binding to E-selectin was tested in the presence or absence of 1 mM CaCl₂. The best binder, IELLQAR, was designated I-peptide.

anti-carbohydrate antibodies that recognize E-selectin ligands or related carbohydrates. Using this approach, we succeeded in identifying a linear 7-mer peptide from a phage display library. Since carbohydrate antigen specificity is determined by 3–4 carbohydrate residues of 600–800 Da, we assumed that a 7-mer peptide of 770 Da would mimic a carbohydrate antigen. The phage library screening yielded a series of peptides with the consensus sequence IXLLXXR [15] (**Figure 1**).

Among those peptides, the strongest binder to E-selectin was IELLQAR, which we designated I-peptide. Chemically synthesized I-peptide inhibited hematogenous colonization of the tumor cells to the lung in mouse [15]. However, in E/P-selectin doubly-deficient mice, tumor cells expressing selectin ligand carbohydrate colonized the lung, and that colonization was inhibited by I-peptide [20]. These results indicated that I-peptide receptor is not an E- or P-selectin and raised the question of what receptor I-peptide bound to in lung vasculature?

To identify the I-peptide receptor, we injected mice intravenously with a biotinylation reagent plus I-peptide-displaying phage or controls. We then isolated lung tissue and immunoprecipitated lysates with rabbit anti-phage antibody or control IgG. When we resolved immunoprecipitates on SDS-PAGE, we detected two *in vivo* biotinylated proteins as 40 kDa and 20 kDa bands on a peroxidase avidin blot (**Figure 2**). We isolated respective candidate receptor proteins from lung membrane fractions using I-peptide affinity chromatography and proteomic analysis and

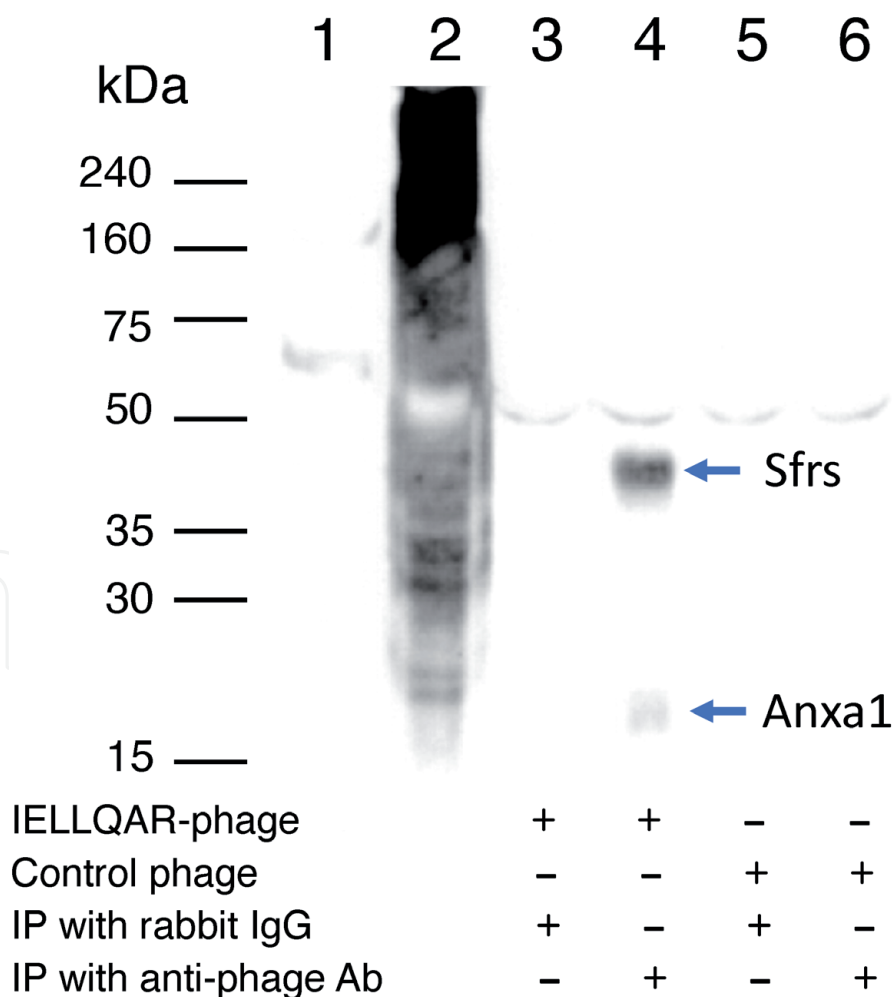


Figure 2.

Detection of I-peptide receptor(s) on the surface of lung endothelial cells by *in vivo* biotinylation. Mice were injected intravenously with either PBS (lane 1) or a biotinylation reagent (lanes 2–6), followed by intravenous injection of I-peptide-displaying (lanes 3 and 4) or control (lanes 5 and 6) phage. After perfusion of mice with PBS, lungs were isolated and phage was immunoprecipitated with rabbit anti-phage antibody (lanes 4 and 6) or rabbit IgG (lane 3 and 5). Immunoprecipitates were resolved on SDS-PAGE and biotinylated proteins detected using a peroxidase avidin blot.

found them to be the pre-mRNA splicing factor (Sfrs) and annexin A1 (Anxa1) [21]. Recombinant Sfrs proteins showed binding to I-peptide and a series of carbohydrates, whose structures overlapped with selectin ligand [21].

Full-length Anxa1 is 37 kDa; therefore, we considered the 20 kDa band seen in **Figure 2** to be a fragment of the full-length protein. By the time we identified Anxa1 fragments, Oh *et al.* had undertaken rigorous subtractive proteomics analysis and identified Anxa1 as a specific vasculature surface marker of malignant tumors [22]. Thus, we hypothesized that I-peptide or related peptides could serve as tumor vasculature-specific drug delivery vehicles via binding to Anxa1. We then rescreened a series of phage clones for tumor-targeting activity and identified an Anxa1-binding, but not Sfrs-binding, phage clone displaying IFLLWQR peptide (**Figure 3**). Moreover, tumor targeting was inhibited in the presence of an anti-Anxa1 antibody specific to the N-terminal region (**Figure 4**) [21].

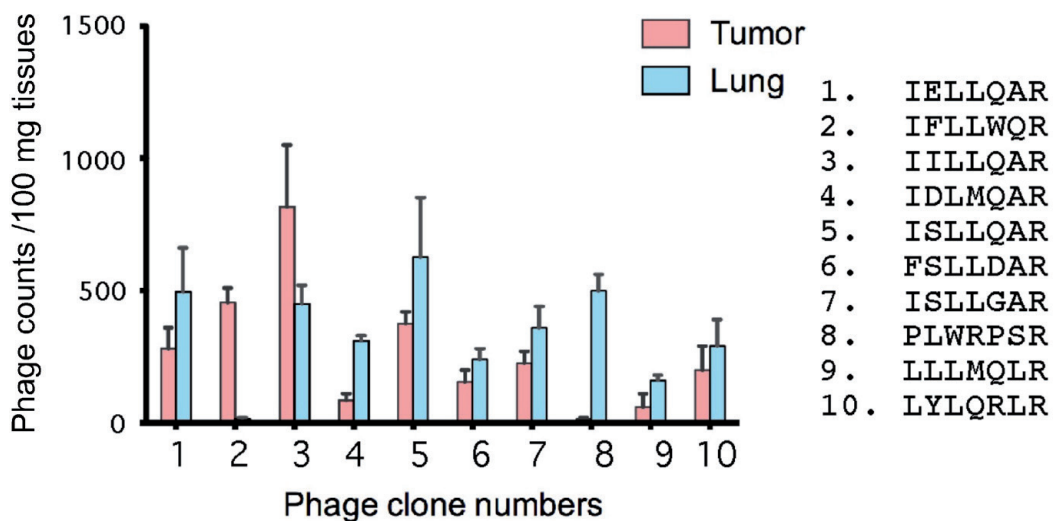


Figure 3.

In vivo phage targeting specificity to tumor and normal lung. Subcutaneous B16 tumor-bearing mice were intravenously injected with each phage clone, and phage number in the tumor and lung was determined by a colony-forming assay. Note that IFLLWQR- or IF7 peptide-displaying phage exclusively targeted the tumor but not lung tissue.

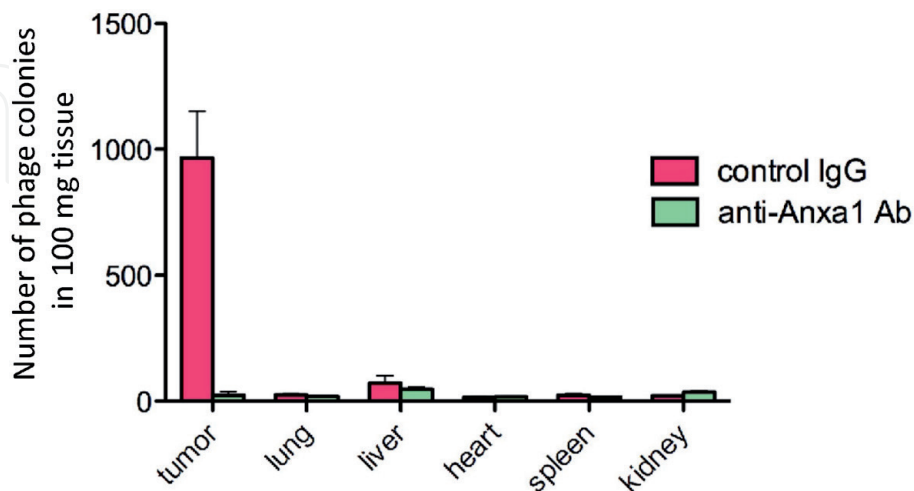


Figure 4.

In vivo tumor and organ targeting by IF7-peptide-displaying phage. IF7-displaying phage were injected intravenously into subcutaneous B16 tumor-bearing mice. Note that IF7-displaying phage targeted the tumor but not normal organs. Tumor targeting by IF7 phage was inhibited by pre-injection of mice with rabbit polyclonal anti-Anxa1 (N-19) antibody directed to the Anxa1 N-terminal domain but not by injection with control rabbit IgG.

3. Targeting the tumor vasculature by IF7 peptide

Next, to visualize tumor targeting by chemically synthesized IF7 peptide, we used intravital microscopy, in which tumor was implanted in a dorsal skinfold chamber [23] visualized tumor vasculature targeting of IF7 under fluorescence microscopy. Green fluorescent Alexa 488-labeled IF7 was injected intravenously and green fluorescent signals were recorded over time by video [14]. Fluorescence appeared in the tumor within 30 sec of injection and increased over time (Figure 5). Analysis of tumor tissue sections taken 15 minutes after A488-IF7 injection indicated fluorescent signals as a punctate staining pattern over endothelial cells (Figure 6, upper). By 40 min, green fluorescence had moved to the stroma (Figure 6, lower), suggesting that IF7 passed through endothelial cells and penetrated the tumor stroma where cancer cells reside. The punctate appearance of Alexa 488 staining suggests that IF7-bound to Anxa1 is internalized by endothelial cells, possibly in vesicles. Anxa1 on the tumor vasculature surface reportedly localizes in caveolae and, when bound by anti-Anxa1 antibody, the complex is internalized into vesicles transported to the basal surface via transcytosis [24]. Accordingly, we concluded that IF7 bound to Anxa1 on the tumor vasculature was transported from the luminal surface to the basal membrane via transcytosis through endothelial cells and likely released to the tumor stroma. Therefore, we asked whether IF7-conjugated chemotherapeutics could cross the BBB to deliver a cytotoxic drug to brain stroma.

To test this possibility we injected A488-IF7 through the tail vein into brain tumor-bearing mice and then prepared sections of mouse brain tissue 20 minutes later. Fluorescence microscopy analysis revealed bright fluorescence in tumor tissue [25]. At higher magnification A488-IF7 fluorescent signals were evident in cytoplasm and/or nuclei of cancer cells. Micrographs of representative organs from the same mouse showed no significant fluorescent signals in normal organs. Brain tumors and representative organs from an animal injected with A488-C(RR) peptide control showed background fluorescence. These results strongly suggest that intravenously-injected IF7 crosses the BBB to target and penetrate brain tumor vasculature and reach cancer cells [25].

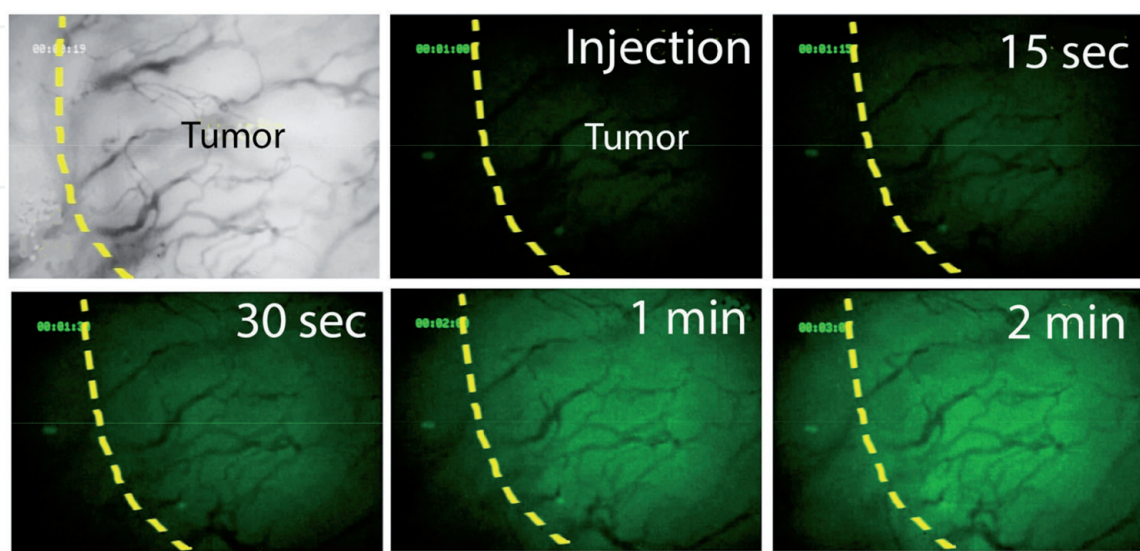


Figure 5. Intravital microscopy of Alexa 488-conjugated IF7 peptide. Mouse lung carcinoma LL/2 tumors were inoculated in the skin of nude mice of a dorsal skin-fold chamber [23]. A488-IF7 was injected intravenously and green fluorescent signals were video-recorded and detected at the indicated times.

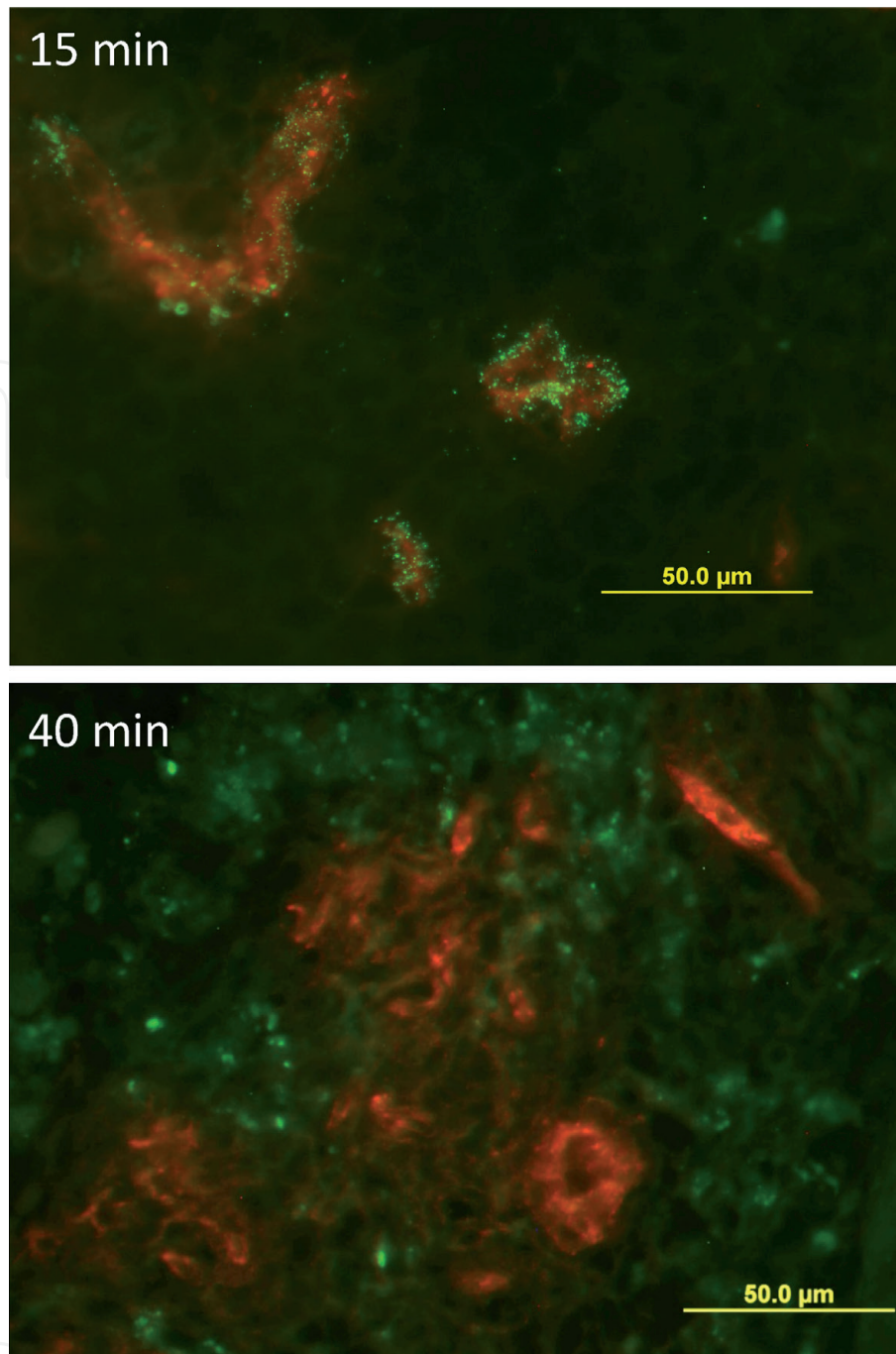


Figure 6. Fluorescence micrograms of subcutaneous B16 tumor sections from mice intravenously-injected with A488-IF7. Tissue sections taken at 15 (upper) and 40 (lower) min after A488-IF7 injection were stained by anti-CD34 antibody plus red fluorescence-conjugated secondary antibody to mark endothelial cells. Note that at 15 min, green IF7 signals are seen as punctate signals over endothelial cells, whereas at 40 min IF7 signals are in the stroma and seen as diffuse green fluorescence.

4. The ANXA1 N-terminal domain is present on the tumor vasculature surface

Several lines of evidence suggest that IF7 binds to human and mouse Anxa1 at the N-terminal domain. First, an IF7 peptide-displaying phage clone failed to bind full-length recombinant ANXA protein when the N-terminus was blocked by a His6-tag, whereas IF7 bound to full-length ANXA1 that was C-terminally tagged with His6 [14]. Second, IF7 bound to full-length ANXA1 but not to an N-terminal deletion delta 27 mutant [14]. Third, when IF7 peptide-displaying phage was injected intravenously into a tumor-bearing mouse, phage targeted the tumor

vasculature, but that binding was blocked in comparable mice injected with an antibody raised against the ANXA1 N-terminal domain (**Figure 4**) [14]. Finally, *in vitro* binding assays showed that synthetic IF7 bound to a synthetic peptide representing the ANXA1 N-terminal domain (designated MC16), which includes 15 amino acids from Met¹ to Glu¹⁵, plus a C-terminal Cys [25]. IF7 bound to both mouse and human MC16 peptides.

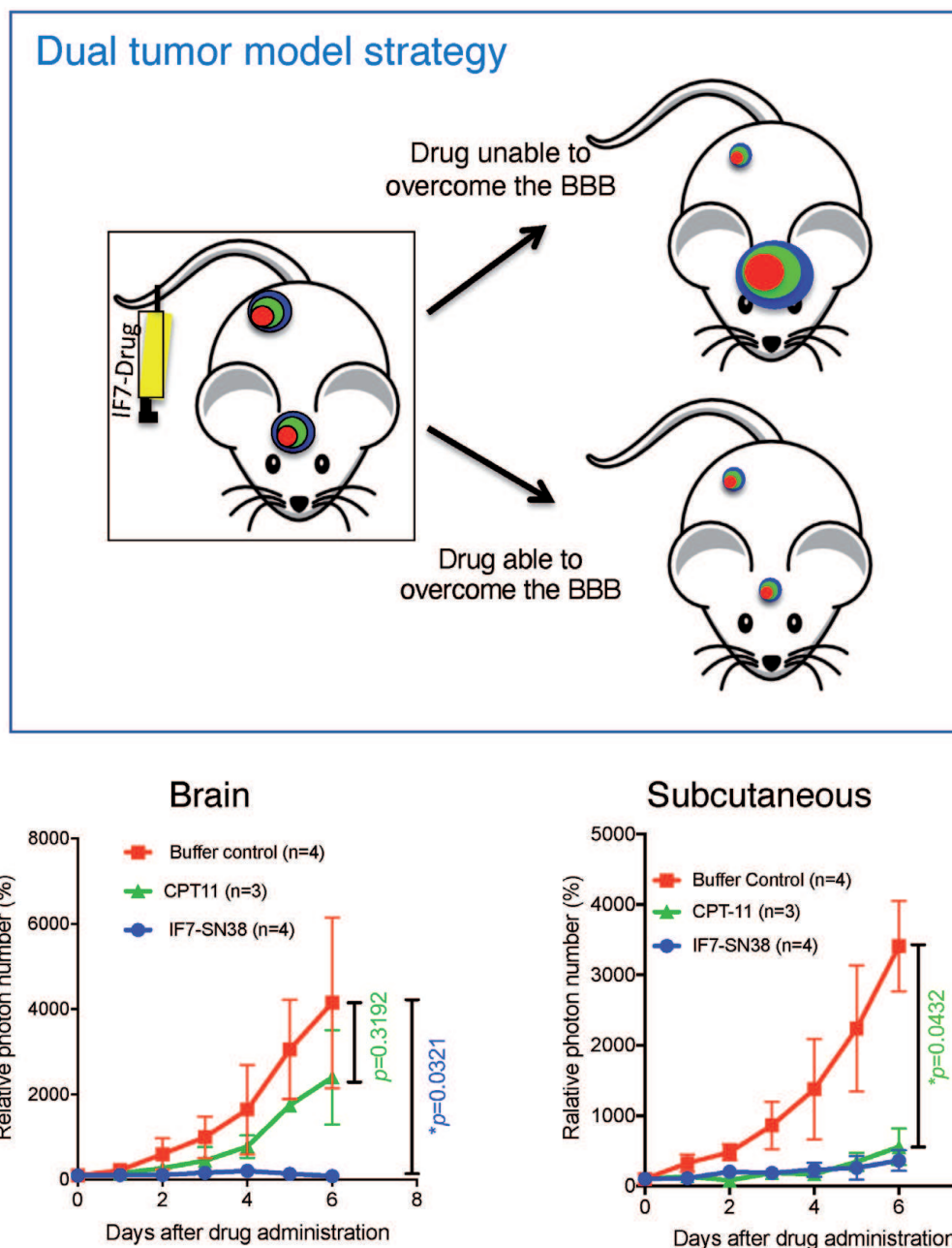
The molecular weight of full-length Anxa1 is 37 kDa, but Western blotting of endothelial plasma membranes and caveolae isolated from tumors detected a 34 kDa band [24]. Proteomics analysis of this 34 kDa protein suggested that it may lack the N-terminal domain. To determine whether the Anxa1 N-terminal domain is on the tumor vasculature surface, we generated a mouse monoclonal antibody specific to the human ANXA1 N-terminal domain (or MC16 peptide). Immunohistochemical analysis of various clinical specimens with anti-MC16 antibody revealed positive signals located at endothelial cells lining malignant tumor tissues in specimens from prostate, breast, lung, liver, ovarian and brain cancers [25], indicating that the ANXA1 N-terminus is present on endothelial cells in many human malignancies. Immunostaining alone did not reveal whether the antigen was on the cell surface or in the cytoplasm.

We confirmed that the MC16 domain was present on the luminal side of the plasma membrane by *in vivo* biotinylation of mouse brain tumors followed by immunoprecipitation by anti-MC16 antibody and proteomics analysis [25]. Plate binding assays of precipitates indicated high levels of biotinylated materials bound by the anti-MC16 antibody in tumor lysates, whereas biotinylated materials in tumor lysates treated with control antibody or those from normal liver tissue lysates showed significantly lower levels of biotinylated material. However, when immunoprecipitates from these tumors were analyzed on a protein gel followed by an avidin blot, we did not detect biotinylated proteins, whereas proteomics analysis had revealed predominantly Anxa1 peptide fragments [25]. We conclude that the Anxa1 N-terminal domain is cleaved from the rest of the protein and displayed on the tumor vasculature surface as a peptide fragment too small to be detected on a Western blot.

5. Therapeutic activity of IF7 conjugated to the anti-cancer drug SN-38 against brain tumors

Both we and others have reported that IF7-conjugated drugs show efficient anti-tumor activity in mouse models of tumors other than brain tumors. Examples include IF7-conjugated geldanamycin (GA) against prostate, lung, and breast cancers as well as melanoma [21], IF7-SN38 against colon cancer [21], IF7-taxol against breast cancer [26] and IF7-conjugated¹⁰B with boron neutron capture therapy against bladder carcinoma [27]. Below we focus on our studies of the effect of IF7-SN38 on mouse brain tumor models.

To target brain tumors, we chose to conjugate IF7 to SN-38, the active component of irinotecan (CPT-11), which is used clinically to treat brain cancer [28, 29]. To compare IF7-SN38 dosages we employed a dual-tumor model, in which a single mouse receives luciferase gene-transfected cancer cells in brain and under the skin (**Figure 7**). Growth of tumors in both regions was quantitatively monitored using an IVIS imager to detect photon numbers produced by luciferase. Once tumors were formed in the brain and under the skin, the dual tumor model mice were injected intravenously with IF7-SN38 and tumor growth in both locations was assessed *in vivo* by photon number. IF7-SN38 treatment significantly suppressed tumor growth relative to buffer controls in both brain and under the skin at a dosage of

**Figure 7.**

Analysis of whether IF7-SN38 overcomes the blood–brain barrier using a dual tumor mouse model. (upper) schematic showing that single mice established to harbor both brain and subcutaneous tumors are injected with IF7-conjugated drug through the tail vein. If the drug cannot overcome the BBB, only subcutaneous tumors are eradicated; if drug overcomes the BBB, growth of both is suppressed. (lower) graphs show that daily injection of IF7-SN38 (7.0 $\mu\text{moles/kg}$) suppressed both brain (left) and subcutaneous (right) tumor growth. Moreover, CPT-11, the SN-38 pro-drug, suppressed growth of subcutaneous tumors at high dosage (50 $\mu\text{moles/kg}$) [25].

3.15 $\mu\text{moles/kg}$. Moreover we found using either C6-Luc cells in SCID mice or B16-Luc cells in C57BL/6 mice, intravenously-injected IF7-SN38 significantly antagonized growth of brain and subcutaneous tumors relative to controls at a dosage of 7.0 $\mu\text{moles/kg}$. When we performed similar experiments using the SN38 prodrug irinotecan alone at doses as high as 50 $\mu\text{moles/kg}$, irinotecan suppressed subcutaneous tumor growth but only minimally suppressed brain tumor growth. Overall, these results indicate that in the mouse dual tumor models tested here, IF7-SN38 suppresses brain tumor growth as effectively as subcutaneous tumor growth.

For the dual tumor model experiments (**Figure 7**), we had dissolved IF7-SN38 in Cremophore EL, a non-ionic detergent used clinically to administer taxol, prior to injection. However, there are concerns about potential inflammatory effects of this detergent [30, 31]. Thus, we conducted experiments in which we dissolved

IF7-SN38 in 10% Solutol HS15, a non-ionic surfactant with low toxicity. The therapeutic effect of IF7-SN38 in 10% Solutol HS15 improved significantly relative to administration with Cremophore EL (**Figure 8A**): B16 brain tumors began shrinking during the first week of daily injections at dosages as low as 2.5 $\mu\text{moles/kg}$, continued shrinking during the second week without drug injection, and then completely disappeared. Mice survived for more than 3 months after cessation of drug treatment without showing signs of B16-Luc cell growth in brain or other parts of their body, suggesting complete remission and potential involvement of host immune systems.

Relevant to potential immunogenicity, when we injected cells of either one of two isogenic lines, B16-Luc or LL/2-Luc, subcutaneously into naïve C57BL/6 mice, both lines produced tumors at injected site. By contrast, when either of these lines were injected into mice that had recovered from brain B16-Luc tumors, LL/2-Luc tumors grew but B16-Luc tumors did not (**Figure 8B**). The presence of tumor-infiltrating lymphocytes, especially CD8⁺ cytotoxic T cells, is correlates with better

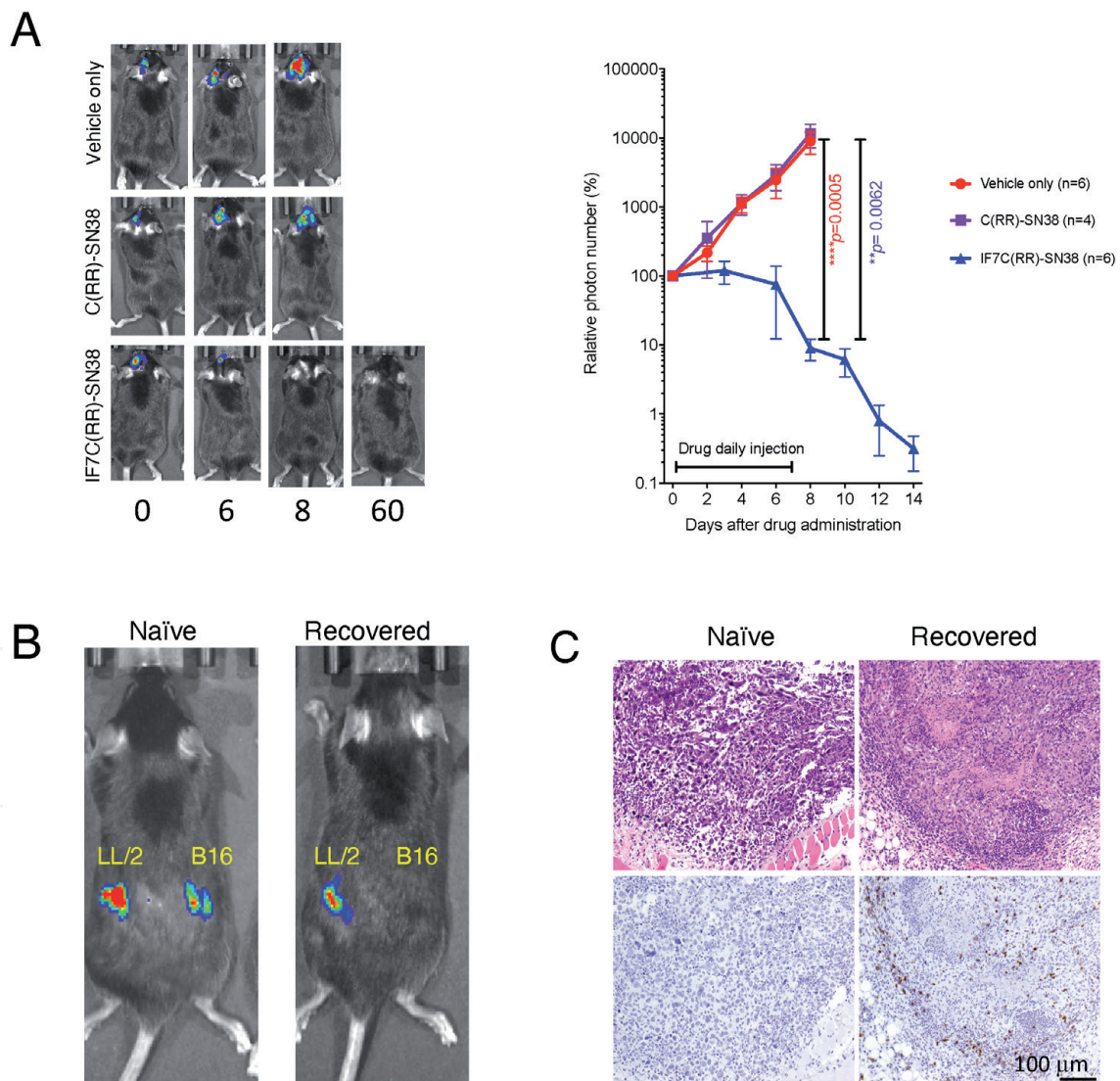


Figure 8. IF7-SN38 treatment promotes complete remission of B16 brain tumors and a host immune response against tumor cells. (A) Effect of IF7-SN38 on B16-Luc brain tumors in isogenic C57BL/6 mice. Drug dosage was 2.5 $\mu\text{moles/kg}$ each for IF7-SN38 and control C(RR)-SN38 diluted with 10% Solutol HS15 in water and administered daily for 7 days. Note that brain tumors continued shrinking after cessation of IF7-SN38 administration in C57BL/6 mice. (B) Growth of two syngeneic cancer lines in naïve and brain-tumor-recovered mice 4 days after subcutaneous injection of LL/2-Luc and B16-Luc cells. (C) Immunohistochemistry with anti-CD8 antibody of B16-Luc cells at subcutaneous injection sites, 20 hours after B16-Luc cell injection.

prognosis of various cancers [32, 33]. Immunohistochemistry of subcutaneous B16-Luc injection site using an anti-CD8 antibody 20 hours after injection of naïve C57BL/6 mice with B16-Luc cells revealed a minimal number of CD8⁺ T cells at challenged sites. By contrast, we observed significant CD8⁺ cell infiltration at injection sites of B16-Luc cells in C57BL/6 mice that had recovered from B16-Luc brain tumors following IF7-SN38 treatment (**Figure 8C**). Thus it is likely that IF7-SN38 therapy leads to complete remission in part by promoting immunological rejection of tumor cells by the host, preventing tumor recurrence elsewhere in the body.

6. Clinical application of IF7-SN38

As described, in mouse the Anxa1 N-terminal domain is present on the surface of tumor vasculature as peptide fragments. Nonetheless, such fragments should serve an IF7 receptor, as either the first 15 amino acid residues of ANXA1 or synthetic MC16 peptide is sufficient for IF7 binding [25]. IF7 binds both human and mouse MC16 peptides equally, suggesting that our results with IF7 in mouse tumor models are relevant to humans.

Although IF7-conjugated drugs are effective in various cancer types [14, 26, 27], their effectiveness against brain malignancies may be particularly high as gene expression data indicates *ANXA1* overexpression in brain tumors [34, 35], a finding supported by immunohistochemistry with anti-MC16 antibody [25]. Moreover, as IF7 targets tumor vasculature and overcomes the BBB, IF7-conjugated drug would accumulate in brain tumor cells, a critical advantage over low molecular weight drugs like temozolomide, which does not target brain tumors and must be administered at high doses (**Figure 9**).

We found the effective dosage of IF7-SN38 in the mouse brain tumor models to be 2.5 μ moles (5.35 mg)/kg (**Figure 8**), which translates into a human equivalent [36] of 0.43 mg/kg or SN-38 0.079 mg. This dosage is considerably lower than that currently recommended for CPT-11 (the SN-38 pro-drug) administered to cancer patients, namely, 120 ~ 200 mg/m² or 2.91 ~ 4.85 mg/kg [37, 38]. Anticipated doses of IF7-SN38 in humans are also unlikely to be toxic at pharmacologically active dosage.

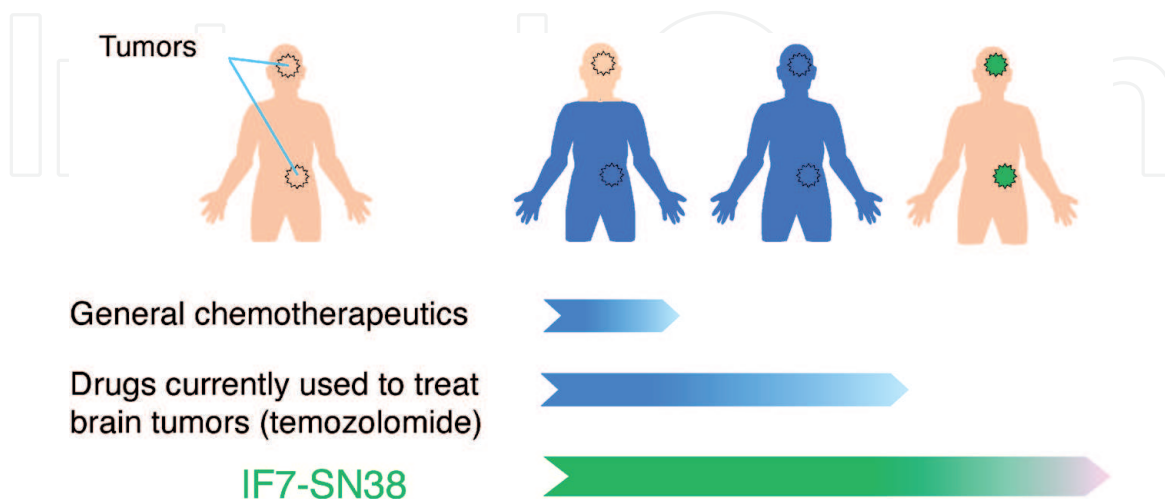


Figure 9.

Mode of action of chemotherapeutics directed against brain tumors. General chemotherapeutics do not penetrate brain tumors due to the BBB and thus are administered to patients at high dosage. Some low molecular weight chemotherapeutics such as temozolomide penetrates the brain but requires high dosage, because temozolomide does not target brain tumors. IF7-SN38 targets brain tumors and overcomes the BBB. At low dosage, IF7-SN38 becomes concentrated in tumors, including brain tumors, and exhibits therapeutic activity.

7. Conclusions and future perspectives

Historically, reagents like IF7 emerged with the advent of carbohydrate mimetic peptides [15, 16]. The surprising finding that Anxa1 is an I-peptide receptor led us to identify IF7 [14, 21]. When IF7 was injected intravenously into brain tumor-bearing mice, it targeted tumor vasculature by binding the Anxa1 N-terminal domain and then crossed the vasculature via transcytosis, to overcome the BBB. Due to its highly specific tumor vasculature targeting activity, IF7-SN38 eradicated brain tumors at low dosage, initiating an immune reaction against cancer cells, followed by complete remission of brain tumors [25]. A similar host immune reaction was also found in IF7-conjugated boron neutron capture therapy in a mouse bladder carcinoma model [27].

IF7-SN38 is, however, susceptible to esterases and proteases. To circumvent stability issues, we have developed an ANXA1-binding D-peptide, designated dTIT7 [39]. We have found that GA-dTIT7, in which geldanamycin is conjugated to dTIT7 through an esterase-resistant linker, is orally administrable and suppresses brain tumor growth in the mouse.

Cancer treatments are increasingly expensive due to development of sophisticated diagnostics and therapies. IF7-SN38 can be chemically synthesized cost-effectively and is stable as a dry powder. Furthermore, orally-administrable peptide-conjugated drugs would be advantageous in societies that lack infrastructure required for costly treatment. Further development of peptide-conjugated drugs could reveal additional candidates with clinical applications against intractable cancers.

Acknowledgements

We thank Dr. Elise Lamar for her editing of the manuscript.

Conflict of interest

The authors declare no conflict of interest.

Author details

Michiko N. Fukuda*, Misa Suzuki-Anekoji and Motohiro Nonaka
Sanford-Burnham-Prebys Medical Discovery Institute, California, USA

*Address all correspondence to: michiko@sbpdiscovery.org

IntechOpen

© 2021 The Author(s). Licensee IntechOpen. This chapter is distributed under the terms of the Creative Commons Attribution License (<http://creativecommons.org/licenses/by/3.0>), which permits unrestricted use, distribution, and reproduction in any medium, provided the original work is properly cited. 

References

- [1] Abbott NJ, Patabendige AA, Dolman DE, Yusof SR, Begley DJ. Structure and function of the blood-brain barrier. *Neurobiol Dis.* 2010;37(1):13-25. doi: 10.1016/j.nbd.2009.07.030. PubMed PMID: 19664713.
- [2] Pardridge WM. The blood-brain barrier: bottleneck in brain drug development. *NeuroRx.* 2005;2(1):3-14. doi: 10.1602/neurorx.2.1.3. PubMed PMID: 15717053; PubMed Central PMCID: PMC539316.
- [3] Pardridge WM. CNS drug design based on principles of blood-brain barrier transport. *J Neurochem.* 1998;70(5):1781-1792. Epub 1998/05/08. doi: 10.1046/j.1471-4159.1998.70051781.x. PubMed PMID: 9572261.
- [4] Przystal JM, Waramit S, Pranjol MZI, Yan W, Chu G, Chongchai A, et al. Efficacy of systemic temozolomide-activated phage-targeted gene therapy in human glioblastoma. *EMBO Mol Med.* 2019;11(4). Epub 2019/02/28. doi: 10.15252/emmm.201708492. PubMed PMID: 30808679; PubMed Central PMCID: PMC6460351.
- [5] Pesce GA, Klingbiel D, Ribi K, Zouhair A, von Moos R, Schlaeppli M, et al. Outcome, quality of life and cognitive function of patients with brain metastases from non-small cell lung cancer treated with whole brain radiotherapy combined with gefitinib or temozolomide. A randomised phase II trial of the Swiss Group for Clinical Cancer Research (SAKK 70/03). *Eur J Cancer.* 2012;48(3):377-384. Epub 2011/11/19. doi: 10.1016/j.ejca.2011.10.016. PubMed PMID: 22093943.
- [6] Zhu W, Zhou L, Qian JQ, Qiu TZ, Shu YQ, Liu P. Temozolomide for treatment of brain metastases: A review of 21 clinical trials. *World J Clin Oncol.* 2014;5(1):19-27. Epub 2014/02/15. doi: 10.5306/wjco.v5.i1.19. PubMed PMID: 24527399; PubMed Central PMCID: PMC3920177.
- [7] Spencer BJ, Verma IM. Targeted delivery of proteins across the blood-brain barrier. *Proc Natl Acad Sci U S A.* 2007;104(18):7594-7599. doi: 10.1073/pnas.0702170104. PubMed PMID: 17463083; PubMed Central PMCID: PMC1857226.
- [8] Hui EK, Boado RJ, Pardridge WM. Tumor necrosis factor receptor-IgG fusion protein for targeted drug delivery across the human blood-brain barrier. *Mol Pharm.* 2009;6(5):1536-1543. Epub 2009/07/25. doi: 10.1021/mp900103n. PubMed PMID: 19624167.
- [9] Sugahara KN, Teesalu T, Karmali PP, Kotamraju VR, Agemy L, Greenwald DR, et al. Coadministration of a tumor-penetrating peptide enhances the efficacy of cancer drugs. *Science.* 2010;328(5981):1031-1035. Epub 2010/04/10. doi: science.1183057 [pii] 10.1126/science.1183057. PubMed PMID: 20378772.
- [10] Agemy L, Friedmann-Morvinski D, Kotamraju VR, Roth L, Sugahara KN, Girard OM, et al. Targeted nanoparticle enhanced proapoptotic peptide as potential therapy for glioblastoma. *Proc Natl Acad Sci U S A.* 2011. Epub 2011/10/05. doi: 1114518108 [pii] 10.1073/pnas.1114518108. PubMed PMID: 21969599.
- [11] Bhaskar S, Tian F, Stoeger T, Kreyling W, de la Fuente JM, Grazu V, et al. Multifunctional Nanocarriers for diagnostics, drug delivery and targeted treatment across blood-brain barrier: perspectives on tracking and neuroimaging. *Part Fibre Toxicol.* 2010;7:3. doi: 10.1186/1743-8977-7-3. PubMed PMID: 20199661; PubMed Central PMCID: PMC2847536.

- [12] Zhou Y, Peng Z, Seven ES, Leblanc RM. Crossing the blood-brain barrier with nanoparticles. *J Control Release*. 2018;270:290-303. Epub 2017/12/23. doi: 10.1016/j.jconrel.2017.12.015. PubMed PMID: 29269142.
- [13] Dhermain FG, Hau P, Lanfermann H, Jacobs AH, van den Bent MJ. Advanced MRI and PET imaging for assessment of treatment response in patients with gliomas. *Lancet Neurol*. 2010;9(9):906-920. Epub 2010/08/14. doi: 10.1016/S1474-4422(10)70181-2. PubMed PMID: 20705518.
- [14] Hatakeyama S, Sugihara K, Shibata TK, Nakayama J, Akama TO, Tamura N, et al. Targeted drug delivery to tumor vasculature by a carbohydrate mimetic peptide. *Proc Natl Acad Sci U S A*. 2011;108(49):19587-19592. Epub 2011/11/25. doi: 1105057108 [pii] 10.1073/pnas.1105057108. PubMed PMID: 22114188; PubMed Central PMCID: PMC3241764.
- [15] Fukuda MN, Ohyama C, Lowitz K, Matsuo O, Pasqualini R, Ruoslahti E, et al. A peptide mimic of E-selectin ligand inhibits sialyl Lewis X-dependent lung colonization of tumor cells. *Cancer Res*. 2000;60(2):450-456. PubMed PMID: 10667600.
- [16] Fukuda MN. Peptide-displaying phage technology in glycobiology. *Glycobiology*. 2012;22(3):318-325. Epub 2011/09/21. doi: cwr140 [pii] 10.1093/glycob/cwr140. PubMed PMID: 21930649; PubMed Central PMCID: PMC3267529.
- [17] Ohyama C, Tsuboi S, Fukuda M. Dual roles of sialyl Lewis X oligosaccharides in tumor metastasis and rejection by natural killer cells. *Embo J*. 1999;18(6):1516-1525. PubMed PMID: 10075923.
- [18] Kannagi R. Carbohydrate-mediated cell adhesion involved in hematogenous metastasis of cancer. *Glycoconj J*. 1997;14(5):577-584. PubMed PMID: 9298690.
- [19] Kannagi R, Izawa M, Koike T, Miyazaki K, Kimura N. Carbohydrate-mediated cell adhesion in cancer metastasis and angiogenesis. *Cancer Sci*. 2004;95(5):377-384. PubMed PMID: 15132763.
- [20] Zhang J, Nakayama J, Ohyama C, Suzuki M, Suzuki A, Fukuda M, et al. Sialyl Lewis X-dependent lung colonization of B16 melanoma cells through a selectin-like endothelial receptor distinct from E- or P-selectin. *Cancer Res*. 2002;62(15):4194-4198. PubMed PMID: 12154017.
- [21] Hatakeyama S, Sugihara K, Nakayama J, Akama TO, Wong SM, Kawashima H, et al. Identification of mRNA splicing factors as the endothelial receptor for carbohydrate-dependent lung colonization of cancer cells. *Proc Natl Acad Sci U S A*. 2009;106(9):3095-3100. PubMed PMID: 19218444; PubMed Central PMCID: PMC264266.
- [22] Oh P, Li Y, Yu J, Durr E, Krasinska KM, Carver LA, et al. Subtractive proteomic mapping of the endothelial surface in lung and solid tumours for tissue-specific therapy. *Nature*. 2004;429(6992):629-635. PubMed PMID: 15190345.
- [23] Lehr HA, Leunig M, Menger MD, Nolte D, Messmer K. Dorsal skinfold chamber technique for intravital microscopy in nude mice. *Am J Pathol*. 1993;143(4):1055-1062. PubMed PMID: 7692730.
- [24] Oh P, Testa JE, Borgstrom P, Witkiewicz H, Li Y, Schnitzer JE. In vivo proteomic imaging analysis of caveolae reveals pumping system to penetrate solid tumors. *Nat Med*. 2014;20(9):1062-1068. doi: 10.1038/nm.3623. PubMed PMID: 25129480.

- [25] Nonaka M, Suzuki-Anekoji M, Nakayama J, Mabashi-Asazuma H, Jarvis DL, Yeh JC, et al. Overcoming the blood-brain barrier by Annexin A1-binding peptide to target brain tumours. *Br J Cancer*. 2020;123(11):1633-1643. Epub 2020/09/15. doi: 10.1038/s41416-020-01066-2. PubMed PMID: 32921792.
- [26] Yu DH, Liu YR, Luan X, Liu HJ, Gao YG, Wu H, et al. IF7-Conjugated Nanoparticles Target Annexin 1 of Tumor Vasculature against P-gp Mediated Multidrug Resistance. *Bioconj Chem*. 2015;26(8):1702-1712. Epub 2015/06/16. doi: 10.1021/acs.bioconjchem.5b00283. PubMed PMID: 26076081.
- [27] Yoneyama T, Hatakeyama S, Sutoh-Yoneyama M, Yoshiya T, Uemura T, Ishizu T, et al. Tumor vasculature-targeted (10)B delivery by an Annexin A1-binding peptide boosts effects of boron neutron capture therapy. *BMC Cancer*. 2021;21(1):72. Epub 2021/01/16. doi: 10.1186/s12885-020-07760-x. PubMed PMID: 33446132; PubMed Central PMCID: PMC7809749.
- [28] Prados MD, Lamborn K, Yung WK, Jaeckle K, Robins HI, Mehta M, et al. A phase 2 trial of irinotecan (CPT-11) in patients with recurrent malignant glioma: a North American Brain Tumor Consortium study. *Neuro Oncol*. 2006;8(2):189-193. doi: 10.1215/15228517-2005-010. PubMed PMID: 16533878; PubMed Central PMCID: PMC1871932.
- [29] Kuroda J, Kuratsu J, Yasunaga M, Koga Y, Saito Y, Matsumura Y. Potent antitumor effect of SN-38-incorporating polymeric micelle, NK012, against malignant glioma. *Int J Cancer*. 2009;124(11):2505-11. Epub 2009/02/04. doi: 10.1002/ijc.24171. PubMed PMID: 19189401.
- [30] Weiss RB, Donehower RC, Wiernik PH, Ohnuma T, Gralla RJ, Trump DL, et al. Hypersensitivity reactions from taxol. *J Clin Oncol*. 1990;8(7):1263-1268. Epub 1990/07/11. doi: 10.1200/JCO.1990.8.7.1263. PubMed PMID: 1972736.
- [31] Gelderblom H, Verweij J, Nooter K, Sparreboom A. Cremophor EL: the drawbacks and advantages of vehicle selection for drug formulation. *Eur J Cancer*. 2001;37(13):1590-1598. Epub 2001/08/31. PubMed PMID: 11527683.
- [32] Salgado R, Loi S. Tumour infiltrating lymphocytes in breast cancer: increasing clinical relevance. *Lancet Oncol*. 2018;19(1):3-5. Epub 2017/12/14. doi: 10.1016/S1470-2045(17)30905-1. PubMed PMID: 29233560.
- [33] Savas P, Salgado R, Denkert C, Sotiropoulos C, Darcy PK, Smyth MJ, et al. Clinical relevance of host immunity in breast cancer: from TILs to the clinic. *Nat Rev Clin Oncol*. 2016;13(4):228-241. Epub 2015/12/17. doi: 10.1038/nrclinonc.2015.215. PubMed PMID: 26667975.
- [34] Sun L, Hui AM, Su Q, Vortmeyer A, Kotliarov Y, Pastorino S, et al. Neuronal and glioma-derived stem cell factor induces angiogenesis within the brain. *Cancer Cell*. 2006;9(4):287-300. doi: 10.1016/j.ccr.2006.03.003. PubMed PMID: 16616334.
- [35] Bredel M, Bredel C, Juric D, Harsh GR, Vogel H, Recht LD, et al. Functional network analysis reveals extended gliomagenesis pathway maps and three novel MYC-interacting genes in human gliomas. *Cancer Res*. 2005;65(19):8679-8689. doi: 10.1158/0008-5472.CAN-05-1204. PubMed PMID: 16204036.
- [36] Nair AB, Jacob S. A simple practice guide for dose conversion between animals and human. *J Basic Clin Pharm*. 2016;7(2):27-31. Epub 2016/04/09. doi: 10.4103/0976-0105.177703. PubMed

PMID: 27057123; PubMed Central
PMCID: PMCPMC4804402.

[37] Stupp R, Hegi ME, Gilbert MR, Chakravarti A. Chemoradiotherapy in malignant glioma: standard of care and future directions. *J Clin Oncol.* 2007;25(26):4127-4136. Epub 2007/09/11. doi: 10.1200/JCO.2007.11.8554. PubMed PMID: 17827463.

[38] Lu CY, Huang CW, Wu IC, Tsai HL, Ma CJ, Yeh YS, et al. Clinical Implication of UGT1A1 Promoter Polymorphism for Irinotecan Dose Escalation in Metastatic Colorectal Cancer Patients Treated with Bevacizumab Combined with FOLFIRI in the First-line Setting. *Transl Oncol.* 2015;8(6):474-9. Epub 2015/12/23. doi: 10.1016/j.tranon.2015.11.002. PubMed PMID: 26692528; PubMed Central PMCID: PMCPMC4700286.

[39] Nonaka M, Mabashi-Asazuma H, Jarvis DL, Yamasaki K, Akama TO, Nagaoka M, et al. Development of an orally-administrable tumor vasculature-targeting therapeutic using annexin A1-binding D-peptides. *PLoS One.* 2021;16(1):e0241157. Epub 2021/01/07. doi: 10.1371/journal.pone.0241157. PubMed PMID: 33406123; PubMed Central PMCID: PMCPMC7787448.